IGNEOUS SEISMIC GEOMORPHOLOGY OF BURIED LAVA FIELDS AND COASTAL ESCARPMENTS ON THE VØRING VOLCANIC RIFTED MARGIN

Sverre Planke(1), John M. Millett(2), Dwarika Maharjan(3), Dougal A. Jerram(4), Mohamed Mansour Abdelmalak(5), Audun Groth(6), Jasper Hoffmann(7), Christian Berndt(8), and Reidun Myklebust(9)

(1) Volcanic Basin Petroleum Research (VBPR), Oslo, Norway, and The Centre for Earth Evolution and Dynamics (CEED), University of Oslo, Norway. Email: planke@vbpr.no.

(2) Volcanic Basin Petroleum Research (VBPR), Oslo, Norway, and Department of Geology and Petroleum Geology, University of Aberdeen, UK. Email: john.millett@vbpr.no.

(3) Volcanic Basin Petroleum Research (VBPR), Oslo, Norway. Email: dwarica@vbpr.no.

(4) DougalEARTH Ltd., Solihull, UK, and The Centre for Earth Evolution and Dynamics (CEED), University of Oslo, Norway. Email: dougal@dougalearth.com.

(5) The Centre for Earth Evolution and Dynamics (CEED), University of Oslo, Norway. Email: m.m.abdelmalak@geo.uio.no.

(6) Statoil, Oslo, Norway. Email: augr@statoil.com.

(7) GEOMAR Helmholtz Centre for Ocean Research Kiel, Germany. Email: jasper_hoffmann@hotmail.de.

(8) GEOMAR Helmholtz Centre for Ocean Research Kiel, Germany. Email: cberndt@geomar.de.

(9) TGS, Asker, Norway. Email: reidun.myklebust@tgs.com.

Original paper date of submission: 30.09.2016

Revised paper date of submission: 07.03.2017

https://mc.manuscriptcentral.com/interpretation
This paper presented here as accepted for publication in Interpretation prior to copyediting and composition.
© 2017 Society of Exploration Geophysicists and American Association of Petroleum Geologists.

ABSTRACT

Voluminous igneous complexes are commonly present in sedimentary basins on volcanic rifted margins, and represent a challenge for petroleum explorationists. A 2500 km^2 industry-standard 3D seismic cube has recently been acquired on the Vøring Marginal High offshore mid-Norway to image sub-basalt sedimentary rocks. This cube also provides a unique opportunity for imaging top- and intra-basalt structures. Detailed seismic geomorphological interpretation of the Top basalt horizon, locally calibrated with high-resolution P-Cable wide-azimuth data, reveal new insight into the late-stage development of the volcanic flow fields and the kilometer high coastal Vøring Escarpment. Subaerial lava flows with compressional ridges and inflated lava lobes cover the marginal high, with comparable structure and size to modern subaerial lava fields. Pitted surfaces, likely formed by lava emplaced in a wet environment, are present in the western part of the study area near the continent-ocean boundary. The prominent Vøring Escarpment formed when eastward-flowing lava reached the coastline. The escarpment morphology is influenced by pre-existing structural highs, and locally these highs are by-passed by the lava. Volcanogenic debris flows are well-imaged on the escarpment horizon, along with large-scale large slump blocks. Similar features exist in active volcanic environments, e.g. on the south cost of Hawaii. Numerous post-volcanic extensional faults and incised channels cut both into the marginal high and the escarpment, and show that the area was geologically active after the volcanism ceased. In summary, igneous seismic geomorphology and seismic volcanostratigraphy are two very powerful methods to understand the volcanic deposits and development of rifted margins. The study demonstrates great promise for further understanding the igneous development of offshore basins as more high-quality 3D seismic data becomes available.

This paper presented here as accepted for publication in Interpretation prior to copyediting and composition.
© 2017 Society of Exploration Geophysicists and American Association of Petroleum Geologists.

INTRODUCTION

There have been major improvements in the intra- and sub-basalt imaging of basalt and sub-basalt sequences in volcanic basins over the past decade (e.g., Abdelmalak et al., 2015; 2016a; 2016b). These improvements have largely been obtained by developments in seismic processing, and in particular by better velocity control, removal of coherent noise such as peg-leg multiples and converted waves, and broadband processing. The advances in processing have been accompanied by improvements in seismic acquisition, including application of new source and receiver technologies and 3D data acquisition in volcanic terrains. The interpretation of volcanic sequences has also improved with the increased availability of high-quality seismic data and fieldwork on analogue seismic-scale outcrops (e.g. Jerram et al., 2009; Planke et al., 2015; Schofield et al., 2016), as well as an understanding of the petrophysics of the volcanic rocks from borehole core and wireline data (e.g. Planke et al., 1999; Japsen et al., 2004; Nelson et al., 2009; Watton et al., 2014; Millett et al., 2015). With these advances in our understanding of volcanic margins, targeted 3D seismic data over key volcanic areas will provide valuable insights into how these margins develop through time and are preserved in the offshore rock record. A high-quality 3D seismic volume and a high-resolution wide-azimuth P-Cable seismic profile were recently acquired on the Vøring Marginal High on the Mid-Norwegian Margin (Figure 1), facilitating detailed mapping of the uppermost basalt sequence.

The Vøring Margin is a type-example of a volcanic rifted margin (Abdelmalak et al., 2016a). The margin was formed by continental breakup between Norway and Greenland. Voluminous basaltic sequences were deposited on both sides of the continent-ocean boundary (COB) during the earliest Eocene (ca. 56-53 Ma; Figure 1). Several kilometer-thick sequences of so-called seaward dipping reflectors (SDR) were imaged on conventional 2D seismic profiles in

This paper presented here as accepted for publication in Interpretation prior to copyediting and composition.
© 2017 Society of Exploration Geophysicists and American Association of Petroleum Geologists.

the 1970's (Hinz, 1981). The SDR sequence was confirmed to be of basaltic nature in the 1980's by the kilometer-deep Ocean Drilling Program Site 642 (Eldholm et al., 1987; 1989). The seismic volcanostratigraphic method was later developed in the 1990's to study the nature, geological history and emplacement of extrusive volcanic rocks from 2D seismic data (Planke et al., 2000) with key volcanic facies within flood basalts also being recognized from the onshore record (e.g. Jerram, 2002). The seismic volcanostratigraphic method is adapted from the concept of seismic stratigraphy (Vail and Mitchum, 1977). Initially, the top and base of the volcanic sequence is mapped. Subsequently, seismic facies units are identified and mapped, and finally interpreted in terms of volcanic facies and emplacement processes using seismic facies analysis. Several characteristic volcanic seismic facies units have been mapped on the Vøring Margin, including the subaerially emplaced SDR and Landward Flows, the coastal Lava Delta, and the subaqueous Inner Flows, Outer High, and Outer SDR (Figure 1b; Berndt et al., 2001). Numerous igneous sheet intrusions, mainly sill complexes, and associated hydrothermal vent complexes, are abundant in the nearby Cretaceous sedimentary basins (Figure 1b; Planke et al., 2005). More recently, new 2D industry seismic profiles have enabled mapping of the overall structure of the volcanic complex, and lead to the division of the Vøring Escarpment into five segments, E1-E5 (Figure 1c; Abdelmalak et al., 2016b). The segmentation of the escarpment is largely controlled by the presence of sub-basalt structural highs and basins and by the shear motion along the Vøring Transform Margin to the southwest. Of particular importance is the central segment E3, where the escarpment is divided into an upper volcanic part of about 200 m high overlying a lower sedimentary part that is almost 1 km high. In this region, the volcanic sequence terminates against a pre-volcanic structural high located along the western flank of the Fenris Basin (Figure

This paper presented here as accepted for publication in Interpretation prior to copyediting and composition.
© 2017 Society of Exploration Geophysicists and American Association of Petroleum Geologists.

1c). This part of the Vøring Escarpment represents a seismic imaging window into the underlying pre-breakup age sedimentary sequences (Abdelmalak et al., 2016b).

Onshore-offshore correlation helps to obtain realistic geological and reservoir models of subsurface seismic data. This process is well developed in sedimentary basins where the construction of reservoir models, using a variety of software packages, is common. Conversely, 3D onshore analogue studies of volcanic margins and flood basalt provinces is still in its infancy. Currently only a handful of seismic models exist for sequences with predominantly volcanic rocks (e.g. Planke et al., 2000). However, investigations from 3D seismic data have recently highlighted the potential for using seismic attribute analysis to improve the imaging of volcanic features such as lava flows in the subsurface (e.g. Thompson, 2005; Thompson and Schofield 2008; Schofield and Jolley, 2013). Early 3D onshore models used logged sections, mapped correlations, satellite data, correlation panels and 3D surface mapping, to construct models of flood basalt and associated sedimentary sequences (e.g. Jerram and Robbe, 2001; Single and Jerram, 2004). More recently the use of 3D Lidar surveying along with high-resolution 3D photogrammetric methods has revolutionized field based 3D surface mapping allowing rapid high precision 3D models to be created with relative ease (e.g. Nelson et al., 2011; Stevenson et al., 2011; Eide et al., 2017).

A 2500 km^2 3D seismic cube was acquired on the central part of the Vøring Marginal High by the petroleum industry in the early 2010's to image potential sub-basalt exploration targets (Figure 1). However, these data also enable a detailed 3D interpretation of the top, base and intra-basalt reflections. The aim of this paper is to study the igneous seismic geomorphology of the Top basalt horizon to better understand the late-stage volcanological development of the Vøring Marginal High and the Vøring Escarpment. The top basalt surface is complex, consisting

This paper presented here as accepted for publication in Interpretation prior to copyediting and composition.
© 2017 Society of Exploration Geophysicists and American Association of Petroleum Geologists.

of primary volcanic deposits subsequently modified by weathering, erosion and deposition of volcanogenic sediments. Seismic geomorphology is described by Posamentier et al. (2007) as "the application of analytical techniques pertaining to the study of landforms and to the analysis of ancient, buried geomorphological surfaces as imaged by 3D seismic data". Igneous seismic geomorphology is defined here as the study of igneous systems (deposits and processes) using 3D seismic images in map view. The geomorphological interpretation is complimented by fieldwork and satellite imagery to gain new insight into the volcanological nature of the seismic observations.

VOLCANOLOGICAL FRAMEWORK

A generalized model for the development of volcanic rifted margins, including the type and distribution of key facies, has been generated from onshore studies (Figure 2). This model considers the evolution of a volcanic margin from onset of initial volcanism to the final rifting phases (e.g. Jerram, 2015). The best-known offshore analogue is the volcanic margin of Norway where the key volcanic seismic facies have been mapped out in detail (Planke et al., 2000; Berndt et al., 2001; Abdelmalak et al., 2016a; 2016b). Integrating onshore and offshore observations through a robust conceptual model comprises a powerful approach for igneous seismic geomorphology.

Initial flood basalt volcanism commonly occurs in a sedimentary basin environment, forming shallow intrusions, peperites, or hydrovolcanic deposits generated by magma-wet sediment interaction, with subaerial lava flows occurring on basin margins and basinal highs (Planke et al., 2000; Wright et al., 2012). Continued flood basalt volcanism leads to more effusive, sub-aerial volcanism where lavas progressively in-fill topographic lows and basins

This paper presented here as accepted for publication in Interpretation prior to copyediting and composition.
© 2017 Society of Exploration Geophysicists and American Association of Petroleum Geologists.

(Millett et al., 2015). If lava reaches an existing shoreline it will fragment in contact with water, constructing a foreset bedded lava delta consisting of hyaloclastites and locally massive flows (Skilling, 2002; Watton et al., 2013). The low strength of these deposits (e.g. Schiffman et al., 2006) and the high-energy coastal environment lead to extensive erosion, slumping, the formation of regional escarpments, and deposition of volcaniclastic sediments by gravity mass flows (e.g. Cannon and Bürgmann, 2001).

The 3D conceptual model in Figure 2 explains the known volcanic seismic facies units (e.g. Inner Flows, Lava Delta, Landward Flows as labelled in Figures 1 and 2). In this scenario the Inner Flows represent an aggradational bottom-set consisting of volcaniclastic sediments mixed with pillow-basalt and massive sheet flows (e.g., Nehyba and Nyvlt, 2015). Lava Deltas are recognized by prograding internal architecture (e.g., Wright et al., 2012) whereas the Landward Flows form sheets of stacked subaerial lavas which transition into Lava Delta facies at the escarpment (e.g. Figure 2).

Both during and after active volcanism, the erupted volcanic material may be modified by erosion and tectonic processes. Subaerial lava sequences will commonly be associated with fissure faults and ridges caused during emplacement and rifting (e.g., Opheim and Gudmundsson, 1989). These may be further utilized by later structural movements but may also influence the development of drainage systems (e.g., Schofield and Jolley, 2013). Where Lava Deltas reach significant thickness, erosion and slumping may play an important role for the final morphology of parts of the escarpment (Jerram et al., 2009; Wright et al., 2012; Abdelmalak et al., 2016b). The key to the study of the igneous seismic geomorphology, is to investigate both primary volcanic and secondary structural/erosional elements of volcanic terrains in order to

This paper presented here as accepted for publication in Interpretation prior to copyediting and composition.
© 2017 Society of Exploration Geophysicists and American Association of Petroleum Geologists.

develop the best possible model of the subsurface geology and the volcanic emplacement environment.

DATA AND METHODS

The main data available for this study is the 3D seismic cube CVX1101 acquired in exploration license PL527 for Chevron Norge. The data were acquired and processed by CGG Veritas. Acquisition was done using two 4980 cu.in. flip-flop air-gun sources with a 25 m shot point interval and recorded on twelve 8 km streamers with 100 m streamer separation. Processing was completed in 2013, and both time and depth cubes were available for this study. The cube covers 2500 km^2, with a 25 by 12.5 m inline and crossline bin size. The data were released after the license was relinquished in 2015.

In addition, one P-Cable high-resolution wide-azimuth seismic profile was included in this study (Planke and Berndt, 2007). This profile was acquired by WGP Survey in 2015 using a 300 cu.in source and a 12.5 m shot point interval and recorded on sixteen 25 m long streamers with 12.5 m streamer separation. The data were processed by TGS in 2015 as a 2D wide-azimuth stacked seismic profile. Subsequently, a 90-100 m wide 3D swath volume with a bin spacing of 3.125 m was processed at GEOMAR including 2D time migration using the velocities determined for the CVX1101 cube. The processed P-Cable cube is about 70 km long. The bandwidth of the data at the Top basalt level is approximately 10-320 Hz at the -20 dB level, compared with a bandwidth of 3-90 Hz for the conventional 3D data.

Both the time and depth cubes were interpreted using the DUG Insight software, but most of the figures in this paper are from the depth cube. Several seismic horizons were initially

This paper presented here as accepted for publication in Interpretation prior to copyediting and composition.
© 2017 Society of Exploration Geophysicists and American Association of Petroleum Geologists.

picked, including the Seafloor, AA, Top basalt, Base basalt, and Sills. The horizons were picked using manual hunt, with the Seafloor, Top basalt and Sills following reflection peaks, and AA and the Base basalt following reflection troughs. Interpretation was undertaken every 25 crosslines, along with key inlines. The interpretation was then propagated and interpolated to complete the horizon picking. The focus of this paper is the Top basalt reflection. On a broad scale, this horizon is easily identified as a high-amplitude peak in the data, defining the Vøring Marginal High, the Vøring Escarpment and the Inner Flows region (Figure 3). However, detailed picking of the horizons for high-resolution studies was more challenging, in particular where the Top basalt was faulted or eroded. Another challenge was to pick the top of the volcanic deposits in areas where this surface was potentially buried by volcanogenic sediments. The improved high-resolution vertical and spatial imaging of the Top basalt reflection in the P-Cable data (Figure 3b) was used to guide the detailed picking of the horizon.

The interpretation of the volcanic sequence followed the seismic volcanostratigraphic approach of Planke et al. (2000). The volcanic sequence boundaries were defined by the Top and Base basalt reflections. Four main seismic facies units were identified in the study area, the 1) SDR, 2) Landward Flows, 3) Lava Delta, and 4) Inner Flows (Figure 3a). Sub-basalt igneous sheet intrusions were interpreted below the volcanic sequence using the methods of Planke et al. (2015). The interpreted sills are characterized by relatively high-amplitude, low-frequency saucer-shaped reflections with abrupt terminations.

Additional seismic volume and horizon attributes were calculated to assist the interpretation and visualization of the data. Similar analysis has proven effective for visualizing lava flow and drainage characteristics on sub-surface volcanic surfaces (Schofield and Jolley, 2013). The variance cube is useful for visualization and interpretation of steeply dipping

https://mc.manuscriptcentral.com/interpretation
This paper presented here as accepted for publication in Interpretation prior to copyediting and composition.
© 2017 Society of Exploration Geophysicists and American Association of Petroleum Geologists.

boundaries such as faults. Root mean squared (RMS) amplitudes were calculated for the Top basalt horizon, using windows of 15 m above and below (RMS30) and 15 m above and 50 m below (RMS65) the horizon. The different horizon and volume attributes were co-blended in the DUG software. The horizon depth or RMS amplitude data were blended with the variance cube, making only the low coherency values visible as dark gray shades on top of the colored and rendered depth or amplitude data (Figure 4).

The Top basalt horizon was studied using the seismic geomorphological approach of Posamentier et al. (2007). Geomorphology is the study of the origin and evolution of the Earth's surface, whereas seismic geomorphology is the study of buried surfaces imaged in 3D seismic data. In this paper, we focus on the volcanological study of the Top basalt horizon to understand the igneous nature and origin of this seismic horizon. The co-blended RMS amplitude and coherency data were particularly useful for this igneous seismic geomorphological study (Figure 4b).

MARGINAL HIGH SURFACE

Volcanic landscapes comprise a wide range of surface features which hold information about the processes which formed them. The RMS65 Top basalt horizon envelope gives a unique opportunity to visualize the volcanic landscape that existed at the end of volcanism on the Vøring Marginal High and the Vøring Escarpment at c. 55 Ma ago (Abdelmalak et al., 2016b). In this section we compare selected features from the RMS65 Top basalt horizon with field analogues from basaltic volcanic provinces around the world in order to establish the emplacement environment of the succession.

This paper presented here as accepted for publication in Interpretation prior to copyediting and composition.
© 2017 Society of Exploration Geophysicists and American Association of Petroleum Geologists.

A fundamental building block of the subaerial part of basaltic provinces are lava flows. In Figure 5 key examples of lava flow features from the RMS65 Top basalt horizon are compared to onshore analogues from GoogleEarth. The lava flows from the RMS65 Top basalt horizon are delimited by their high amplitudes lobe like margins and comprise a range of morphologies and scales but typically display lava lobes between c. 0.5-2 km wide and thicknesses roughly interpreted to be on the order of a few 10's of meters. There are several examples of curved ridges on the surfaces of lava lobe features from the RMS65 Top basalt horizon. In nature these ridges are formed due to compression of the evolving lava crust as it cools whilst flow of lava continues beneath the insulating crust forming distinct compression or 'ropey' ridges on a range of scales which are curved in the direction of flow (Fink and Fletcher, 1978; Gregg et al., 1998; Ball et al., 2008). Another common feature of basaltic lava flows is the development of multiple flow lobes and anastomosing channels which commonly relate to the development of flow fields fed by continuous to semi-continuous eruptions commonly lasting anywhere from days to decades. In the RMS65 Top basalt horizon, a number of compound to channelized lava flows are observed (Figures 5a-c). Depending on a range of factors including viscosity, temperature, effusion rate, eruption environment etc. lavas may undergo significant inflation resulting in the thickening of the flow lobes (e.g., Figure 5c; Hon et al., 1994; Self et al., 1996). Similar lava flow features have also been imaged within the Faroe-Shetland basin to the SW of the study area (Schofield and Jolley, 2013).

In the western region of the data cube, overlying the feather edge of the SDR domain, a highly pitted and irregular surface is revealed in the RMS65 Top basalt horizon (Figure 5d). The surface reflection comprises high amplitudes similar to lava flows elsewhere in the survey but with numerous sub-rounded to irregular pit-like features with low amplitudes. These pitted

This paper presented here as accepted for publication in Interpretation prior to copyediting and composition.
© 2017 Society of Exploration Geophysicists and American Association of Petroleum Geologists.

surfaces appear to grade smoothly laterally into more typical sheet like lava features implying that they are linked. A number of explanations of these features are possible from observations of volcanic terrains such as pressure ridges or tumuli, hummocky pahoehoe surfaces and deflation structures (e.g. Hon et al., 1994). However, perhaps the best potential analogue are lava flows which have developed extensive rootless or littoral cones which form common features where lavas flow over water saturated surfaces (Hamilton et al., 2010; Reynolds et al., 2015; Noguchi et al., 2016). Such rootless cones form from the explosive interaction between lava flowing over water saturated sediments, lakes, rivers or ponded water. The resulting craters are deeply excavated and partly filled with fragmental volcanic detritus. They would be expected to display reduced velocities compared to the more coherent surrounding lava flow. In Figure 5d an example of the extensive closely spaced rootless cones at Myvatn, Iceland, is shown as a possible analogue. These features are quick to erode which would leave a pock-marked irregular landscape very similar to the RMS65 Top basalt horizon. By implication the RMS65 Top basalt horizon features could therefore represent a lava field which interacted with a wet substrate over large areas which is plausible given its location above the rapidly subsiding SDR domain at the seaward margin of the Vøring Marginal High (Planke et al., 2000). The development of ravinement structures elsewhere on the top basalt (see discussion below) also highlight that river systems were developing on the subaerial lava flows, and provide clear evidence of surface water.

Perhaps one of the most striking features revealed by the RMS30 Top basalt horizon are the fault structures and associated displacements which dissect the palaeo-surface (Figure 6). In Figure 6a lava flow features similar to those highlighted in Figure 5 are observed. Clear lobate lava flow margins and possible pits are also well imaged. The extensional faulting is observed

This paper presented here as accepted for publication in Interpretation prior to copyediting and composition.
© 2017 Society of Exploration Geophysicists and American Association of Petroleum Geologists.

throughout the entire study area and there is no clear evidence of reverse faults. In Figure 6a north-trending graben structures are imaged with a fault spacing of c. 400-500 m and displacements of typically c. 30-50 m. In Figure 6c, the fault traces which dissect the Skoll High Top basalt surface are clearly imaged dissecting the palaeo Vøring Escarpment surface and can be traced across the scarp and through the Inner Flows. In Figure 6d a field analogue from the faulted lava surface of the Reykjanes Peninsula rift zone is displayed.

In Figure 7a, the faulted top basalt RMS65 Top basalt horizon is visualized looking westward across the Skoll High. Clearly meandering erosional channel features are observed cutting the surface across the entire central part of the Landward Flows lava plateau. The main channels are c. 400 m in width and generally c. 30-45 m deep in the deepest parts. The depth of the channels appears to reduce towards the escarpment. Clear tributary channels are observed to join the main channels appearing to originate from within the plateau. At the margins of the channels, traces of terraces step back from the channel.

In Figure 7b, a potential analogue example of two river channels cutting through the Miocene aged Columbia River Basalt Province (CRBP) is presented. The 2D cross-sectional view of the channels is presented in Figure 7c. The features revealed by the RMS65 Top basalt horizon display clear examples of erosional channels cutting the palaeo Landward Flows surface. The channels suggest a significant period of sub-aerial exposure at the end of the main phase of volcanism on the Skoll High. The scale of the drainage systems and their catchments are difficult to infer without constraints on the time it took for them to form, but they clearly demonstrate the development of drainage systems within the lava field (Schofield and Jolley, 2013; Ebinghaus et al., 2014). These channels present clear evidence for drainage systems coming from the west at this time feeding sediments into the Vøring Basin, likely in-filling the Fenris Graben.

https://mc.manuscriptcentral.com/interpretation
This paper presented here as accepted for publication in Interpretation prior to copyediting and composition.
© 2017 Society of Exploration Geophysicists and American Association of Petroleum Geologists.

VØRING ESCARPMENT

The Vøring Escarpment comprises a major structural component of the Norwegian continental margin and formed a prominent topographical feature at the end of the Paleogene volcanism (Abdelmalak et al., 2016b). Figure 8 displays the RMS30 Top basalt horizon across the escarpment in the NE part of the study area near the eastern flank of the Skoll High. A different visualization of the escarpment region is shown in Figure 9. The escarpment is generally on the order of c. 1 km high with a dip of c. 25-30°. High seismic amplitude lava flows transgress across the escarpment edge into spatially coherent aprons of high amplitude chaotic reflectors. These features are interpreted as volcanic debris flows connecting the Landward Flows domain on the marginal high with Inner Flows domain at the basin floor across the escarpment (Figures 8a and 9). The term 'debris flows' is used as a broad description for the extrusive volcaniclastic facies which are observed to flow down the escarpment within the seismic data. In reality these facies can be highly complex and include various hyaloclastites, pillows and feeder tubes (e.g. Watton et al., 2013). In cross section these surface features are clearly linked to classic rifted margin architectural features (Planke et al., 2000). A number of prominent slump structures are also clearly identified at the top of the escarpment (Figure 8). The identification of debris flows draping these perched slump features demonstrates that they formed part of the palaeotopography at the time of volcanism.

The features revealed from the RMS30 Top basalt horizon show clear similarities to present day analogues from e.g. Hawaii (Figure 10). In the Hawaii example, lava flows from Mauna Ulu are observed to flow down the flanks of Mauna Loa across the prominent fault scarps associated with the Hilina fault system (Cannon and Bürgmann, 2001). The faulting in the

This paper presented here as accepted for publication in Interpretation prior to copyediting and composition.
© 2017 Society of Exploration Geophysicists and American Association of Petroleum Geologists.

Hawaii example is related to flank collapse of the Hawaii oceanic island, however, the volcanic features and the geomorphological similarities to the Vøring Escarpment RMS30 Top basalt horizon are striking. Lava delta deposits form highly unstable deposits which are prone to instability and collapse (Schiffman et al., 2006). In the Hawaiian example, lavas enter the ocean through the passage zone (e.g., Skilling, 2002) and transition downslope into lava delta deposits comprising hyaloclastite and pillow breccias. Evidence for extensive and complex slumping and mass wasting of the subsea escarpment is also observed from offshore bathymetric data around Hawaii (Smith et al., 1999).

In Figure 11, the depth and RMS30 Top basalt horizons across the escarpment are displayed for the central portion of the study area. The depth image displays a highly dissected escarpment surface with numerous channel-like features orientated perpendicular to the escarpment. Compared to the RMS30 Top basalt surface, a number of low amplitude regions are clearly observed between, and partly dissected, by the dominantly high amplitude top basalt surface. These low amplitude regions are interpreted to represent sub-cropping pre-volcanic sedimentary units comprising a correlative unconformity to the top basalt surface. This interpretation is supported by the 2D seismic line presented in Figure 11c. The low amplitude regions are only observed below c. 200 m from the top of the escarpment. Along with evidence from Figure 3a, this 200 m interval is interpreted to represent the thickness of the erupted lava sequence in this part of the Skoll High. It should be noted that the thickness of the lavas capping the Vøring Marginal High increases away from the Skoll High to the NE and SW. A present day terrestrial example of a deeply eroded volcanic topped escarpment is presented in Figure 12. Although this forms a subaerial setting, the scale and general geomorphology of the basalt capped escarpment shows clear similarities to the Vøring Escarpment surface.

This paper presented here as accepted for publication in Interpretation prior to copyediting and composition.
© 2017 Society of Exploration Geophysicists and American Association of Petroleum Geologists.

A striking feature of the RMS30 Top basalt horizon in Figure 11b is the relationship between the high-amplitude volcanic facies and the incised escarpment surface. Thin channelized volcanic debris flow facies are observed to flow down the channels on the escarpment surface but are also clearly deflected around the topographic highs formed by the sedimentary subcrops. These lava-fed debris flows clearly post-date the incised channels on the palaeo-escarpment surface and therefore represent late-stage eruptions flowing across the Skoll High. The channelized lava debris flows are clearly observed to spread out into wider sheet like surfaces at the base of the escarpment. It is possible that these features represent the fanning of volcaniclastic debris but they may also represent sub-aqueous sheet flows (e.g., Bartiza and White, 2000) potentially connected to the subaerial Skoll High feeder lavas by lava tubes (Watton et al., 2013).

CONCLUSIONS

This igneous seismic geomorphological study of the Top basalt horizon on a recently acquired 3D seismic cube on the central Vøring Marginal High reveals new documentation and insight into the late-stage development of a ca. 55 Ma old voluminous volcanic sequence. The unique, high-quality cube was interpreted by detailed seismic picking of the Top basalt horizon. The accuracy of the horizon interpretation was enhanced by using a high-resolution P-Cable wide-azimuth profile through the cube. The 3D data were visualized in combination with horizon and volume attributes to enhance the volcanological imaging.

The seismic data in conjunction with fieldwork and satellite imagery revealed for the first time extensive subaerial lava flow fields, lava flows with compressional ridges and inflated lava lobes, and pitted lava surfaces likely formed in a wet environment. The lava fields were

This paper presented here as accepted for publication in Interpretation prior to copyediting and composition.
© 2017 Society of Exploration Geophysicists and American Association of Petroleum Geologists.

subsequently intensively faulted to form graben structures incised by channels transporting sediments into the Fenris Graben.

The steeply dipping (25-30^{o}) kilometer-high Vøring Escarpment was formed by the complex interaction of volcanological and sedimentological processes. Subaerial lava flows are imaged where they entered the sea at the top of the escarpment, with spectacularly well-imaged volcanogenic debris flows deposited downward on the escarpment and on the basin floor. Locally, slump blocks are well-defined in the seismic data.

The escarpment is composed of both volcanic sequences and pre-volcanic sediments in the southern part of the cube. Here, an almost 1 km thick sedimentary sequence, forming a structural high at the time of volcanism, is incised by several channels. Some of these channels were later utilized by subaqueous lava flows. The morphology of the escarpment is very similar to onshore active volcanic environments in Hawaii and inactive great escarpments in South Africa. This suggests that - at least during the late stage of volcanism - the emplacement of flood basalt provinces was governed by the same eruption and flow mechanisms as modern volcanic systems. The major channel systems cutting the top basalt and the escarpment surfaces has implications for sediment (possibly siliciclastic) supply and entry points into outer Vøring Basin.

This study identifies useful workflows for the interpretation of volcanic deposits in seismic data. Following Posamentier et al. (2007), we argue that igneous seismic geomorphology, when used in conjunction with seismic volcanostratigraphy, represents the state of the art approach to extract volcanological insights from 3D seismic data.

ACKNOWLEDGEMENTS

https://mc.manuscriptcentral.com/interpretation
This paper presented here as accepted for publication in Interpretation prior to copyediting and composition.
© 2017 Society of Exploration Geophysicists and American Association of Petroleum Geologists.

We are very grateful for P-Cable data access from TGS and VBPR. We further acknowledge the support from the Research Council of Norway through its Centres of Excellence funding scheme, project 22372. Constructive editorial and anonymous reviews are also greatly appreciated.

FIGURE CAPTIONS

Figure 1. Overview of the volcanic setting of the mid-Norwegian rifted margin and location of the interpreted seismic data. A) Bathymetric map showing the Vøring Plateau (VP), Ocean Drilling Program (ODP) Site 642, and the continent-ocean boundary (COB). B) Schematic cross-section of the Vøring Margin showing characteristic igneous complexes and associated volcanic seismic facies units (Planke et al., 2000). Approximate location shown as yellow line in Figure 1a. C) Regional structural map of the Top basalt horizon on the Vøring Margin slowing the location of the interpreted 3D seismic cube (blue polygon) and P-Cable data (white line, f3). The Vøring Escarpment is divided into five segments, E1 to E5. Structural highs outlined by dashed lines and depth contours in km (gray lines) annotated. Modified from Abdelmalak et al. (2016b). COB: Continent-Ocean Boundary. HTVC: Hydrothermal Vent Complex; K: K-reflection, the base of SDR; SDR: Seaward Dipping Reflectors; VP: Vøring Plateau.

Figure 2. Sketch of volcanic processes and deposits relevant for the Vøring Margin breakup volcanism. Characteristic volcanic seismic facies units (e.g., Inner Flows and Lava Delta) are labeled.

Figure 3. Seismic data examples showing typical data quality. a) Arbitrary seismic profile across the northern part of the 3D survey with interpreted horizons. Line located in Figure 1c. b) Comparison of conventional and high-resolution P-Cable 3D seismic data on the marginal high

This paper presented here as accepted for publication in Interpretation prior to copyediting and composition.
© 2017 Society of Exploration Geophysicists and American Association of Petroleum Geologists.

on time slices (upper panel shows 90 m wide P-Cable swath in green compared with conventional 3D; depth of time slices marked by yellow line below) and seismic sections. c) Vøring Escarpment seismic example, showing comparison of P-Cable and conventional time slices (upper panel; color scheme as in Figure 3b) and P-Cable seismic section (below).

Figure 4. Perspective views of the Top basalt horizon. a) Depth and coherency blend. b) Top basalt RMS amplitude and coherency blend (RMS65). Seismic profiles located (f3, f8, f6, f10).

Figure 5. Comparison between seismic lava flow geomorphology of the RMS65 Top basalt horizon with field analogues. a) Compression ridges formed on the surfaces of lava flows indicating flow direction. b) Compound braided lava lobes formed by the eruption of numerous anastomosing flow lobes. c) Large inflated flow lobes with multiple smaller lobes at margins. d) Pitted irregular lava surfaces formed by the formation of rootless cones where lava erupt over a water saturated substrate. All scale bars represent ~1 km unless stated otherwise. Field images from Google Earth.

Figure 6. Perspective view of faulted lava fields on the RMS30 Top basalt horizon. a) Grabens dissecting the Skoll High viewed from the south. b) The 2D seismic line in a) showing that the faults cut through the volcanic sequence (Landward Flows and Lava Delta). c) Examples of faults dissecting the Vøring Escarpment and the Inner Flows. View from the north. d) Field analogue of a faulted lava field in a rift zone. Seismic profile located in Figure 4.

Figure 7. Examples of erosional channels cutting into the top basalt surface. a) Large meandering channels cutting the RMS65 Top basalt horizon. b) Field analogue from the Columbia River Basalt Province (CRBP) where erosional channels incise the lava plateau. c) 2D

This paper presented here as accepted for publication in Interpretation prior to copyediting and composition.
© 2017 Society of Exploration Geophysicists and American Association of Petroleum Geologists.

seismic line showing the discontinuous Top basalt horizon with incised channels. Line located in Figures 4 and 7a.

Figure 8. Igneous seismic geomorphology of the Vøring Escarpment. a) Perspective view of the RMS30 Top basalt horizon seen from the north. b) Seismic example along the blue line in a). Location of fault scarp (F1) and lava flows (L1, L2) shown. IF: Inner Flows.

Figure 9. Perspective view of the Vøring Escarpment, looking towards SW. The image displays the interpreted Top basalt horizon blended with coherency data. The image reveals a well-developed subaerial lava field on the Vøring Marginal High and a prominent, about 1 km high, coastal escarpment. Volcanogenic debris flows are identified on the escarpment and spreads out as lobes in the Fenris Graben. Note that the Top basalt horizon is picked at a slightly higher stratigraphic level than in Figure 8 in this part of the cube to better visualize the lower part of the debris flow. Scale bar is approximate for the central part of the figure. The image was generated using the Petrel software.

Figure 10. Analogue igneous geomorphology of escarpments in Hawaii. a) Google Earth perspective view of the southern part of Hawaii, showing fault scarps (pali) and recent lava fields. b) Photo of recent lava flows across the fault scarp.

Figure 11. Perspective view of paleo-channels, or valleys, across the Vøring Escarpment. a) Depth horizon of the Top basalt. b) RMS30 Top basalt horizon. c) Seismic strike-line along the central part of the escarpment. Profile located in Figure 4 and as blue line in Figures 10a,b. Numbers 1, 2, and 3 show valleys and ridge. Color scales as in Figure 4.

This paper presented here as accepted for publication in Interpretation prior to copyediting and composition.
© 2017 Society of Exploration Geophysicists and American Association of Petroleum Geologists.

Figure 12. Analogue erosional channels on the southeastern flank of the Lesotho plateau, South Africa. View towards northwest. The elevation of the Sani Pass is from c. 1600-2900 m, with the upper 1000 m comprising lavas overlying the Clarens Sandstone. Image from GoogleEarth.

REFERENCES

Abdelmalak, M. M., T. B. Andersen, S. Planke, J. I. Faleide, F. Corfu, C. Tegner, G. E. Shephard, D. Zastrozhnov, and R. Myklebust, 2015, The ocean-continent transition in the mid-Norwegian Margin: Insight from seismic data and an onshore Caledonian field analogue: Geology, **43**, 1011–1014.

Abdelmalak, M. M., R. Meyer, S. Planke, J. I. Faleide, L. Gernigon, J. Frieling, A. Sluijs, G.-J. Reichart, D. Zastrozhnov, S. Theissen-Krah, A. Said, and R. Myklebust, R., 2016a, Pre-breakup magmatism on the Vøring Margin: Insight from new sub-basalt imaging and results from Ocean Drilling Program Hole 642E: Tectonophysics, **675**, 258-274.

Abdelmalak, M. M., S. Planke, J. I. Faleide, D. A. Jerram, D. Zastrozhnov, S. Eide, and R. Myklebust, 2016b, The development of volcanic sequences at rifted margins: New insights from the structure and morphology of the Vøring Escarpment, mid□Norwegian Margin: Journal of Geophysical Research, Solid Earth, **121**, 5212-5236.

Ball, M., H. Pinkerton, and A. J. L. Harris, 2008, Surface cooling, advection and the development of different surface textures on active lavas on Kilauea, Hawai'i: Journal of Volcanology and Geothermal Research, **173**, 148-156.

This paper presented here as accepted for publication in Interpretation prior to copyediting and composition.
© 2017 Society of Exploration Geophysicists and American Association of Petroleum Geologists.

Berndt, C., S. Planke, E. Alvestad, F. Tsikalas, and T. Rasmussen, 2001, Seismic volcanostratigraphy of the Norwegian Margin: constraints on tectonomagmatic break-up processes: Journal of the Geological Society, **158**, 413-426.

Cannon, E. C., and R. Bürgmann, R, 2001, Prehistoric fault offsets of the Hilina fault system, south flank of Kilauea Volcano, Hawaii: Journal of Geophysical Research, **106**, 4207-4219.

Ebinghaus, A., A. J. Hartley, D. W. Jolley, M. Hole, and J. M. Millett, 2014, Lava–sediment interaction and drainage-system development in a large igneous province: Columbia River Flood Basalt Province, Washington State, USA. Journal of Sedimentary Research, **84**, 1041-1063.

Eide, C. H., N. Schofield, D. A. Jerram, and J. A. Howell, 2017, Basin-scale architecture of deeply emplaced sill complexes: Jameson Land, East Greenland: Journal of the Geological Society, **174**, 23-40.

Eldholm, O., J. Thiede, and E. Taylor, 1989, Evolution of the Vøring Volcanic Margin: Proceedings of the Ocean Drilling Program, Scientific Results, **104**, 1033–1065.

Eldholm, O., J. Thiede, E. Taylor, and S. S. Party, 1987, Summary and preliminary conclusions, Proceedings of the Ocean Drilling Program, Initial Report, **104**, 751–771.

Fink, J. H., and R. C. Fletcher, 1978: Ropy pahoehoe: Surface folding of a viscous fluid: Journal of Volcanology and Geothermal Research, **4**, 151-170.

Gregg, T. K., J. H. Fink, and R. W. Griffiths, 1998, Formation of multiple fold generations on lava flow surfaces: Influence of strain rate, cooling rate, and lava composition: Journal of Volcanology and Geothermal Research, **80**, 281-292.

This paper presented here as accepted for publication in Interpretation prior to copyediting and composition.
© 2017 Society of Exploration Geophysicists and American Association of Petroleum Geologists.

Hamilton, C. W., S. A. Fagents, and T. Thordarson, 2010, Explosive lava–water interactions II: self organization processes among volcanic rootless eruption sites in the 1783–1784 Laki lava flow, Iceland: Bulletin of Volcanology, **72**, 469-485. DOI 10.1007/s00445-009-0331-5.

Hinz, K., 1981, Hypothesis on terrestrial catastrophes: wedges of very thick oceanward dipping layers beneath passive margins-their origin and palaeoenvironement significance: Geologisches Jahrbuch, **22**, 345–363.

Hon, K., J. Kauahikaua, R. Denlinger, and K. Mackay, 1994, Emplacement and inflation of pahoehoe sheet flows: Observations and measurements of active lava flows on Kilauea Volcano, Hawaii: Geological Society of America Bulletin, **106**, 351-370.

Japsen, P., M. S. Andersen, L. O. Boldreel, R. Waagstein, R. S. White, and M. Worthington, 2004, Seismic and petrophysical properties of Faroe Islands basalts: the SeiFaBa project: Geological Survey of Denmark and Greenland Bulletin, **4**, 53–65.

Jerram, D. A., 2002, Volcanology and facies architecture of flood basalts: Volcanic Rifted Margins Special Paper, Geological Society of America, **362**, 119–132.

Jerram, D. A. and O. Robbe, O., 2001, Building a 3-D model of a flood basalt: an example from the Etendeka, NW Namibia: Visual Geosciences, **6**, 1-8.

Jerram, D. A., 2015, Hot rocks and oil: Are volcanic margins the new frontier? Elsevier R&D Solutions for Oil and Gas, Exploration & Production, https://www.elsevier.com/__data/assets/pdf_file/0008/84887/ELS_Geofacets-Volcanic-Article_Digital_r5.pdf

This paper presented here as accepted for publication in Interpretation prior to copyediting and composition.
© 2017 Society of Exploration Geophysicists and American Association of Petroleum Geologists.

Jerram, D. A., R. T. Single, R. W. Hobbs, and C. E. Nelson, 2009, Understanding the offshore flood basalt sequence using onshore volcanic facies analogues: An example from the Faroe-Shetland basin: Geological Magazine, **146**, 353–367.

Millett, J. M., M. J. Hole, D. W. Jolley, N. Schofield, and E. Campbell, 2015, Frontier exploration and the North Atlantic Igneous Province: new insights from a 2.6 km offshore volcanic sequence in the NE Faroe–Shetland Basin: Journal of the Geological Society, **173**, 320-336.

Nehyba, S., and D. Nyvlt, 2015, "Bottomsets" of the lava−fed delta of James Ross Island Volcanic Group, Ulu Peninsula, James Ross Island, Antarctica: Polish Polar Research, **26**, 1-24.

Nelson, C. E., D. A. Jerram, R. W. Hobbs, R. Terrington, and H. Kessler, 2011, Reconstructing flood basalt lava flows in three dimensions using terrestrial laser scanning: Geosphere, **7**, 87-96.

Nelson, C. E., D. A. Jerram, and R. W. Hobbs, 2009, Flood basalt facies from borehole data: implications for prospectivity and volcanology in volcanic rifted margins: Petroleum Geoscience, **15**, 313-324.

Noguchi, R., Á. Höskuldsson, and K. Kurita, 2016, Detailed topographical, distributional, and material analyses of rootless cones in Myvatn, Iceland: Journal of Volcanology and Geothermal Research, **318**, 89-102.

Opheim, J. A., and A. Gudmundsson, 1989, Formation and geometry of fractures, and related volcanism, of the Krafla fissure swarm, northeast Iceland: Geological Society of America Bulletin, **101**, 1608-1622.

This paper presented here as accepted for publication in Interpretation prior to copyediting and composition.
© 2017 Society of Exploration Geophysicists and American Association of Petroleum Geologists.

Planke, S., and C. Berndt, 2007, Apparatus for seismic measurements. U.S. Patent No. 7.221.620.

Planke, S., T. Rasmussen, S. S. Rey, and R. Myklebust, 2005, Seismic characteristics and distribution of volcanic intrusions and hydrothermal vent complexes in the Vøring and Møre basins, *in* Doré, A.G., and B. A. Vining (Eds.), Petroleum Geology: North-West Europe and Global Perspectives-Proceedings of the 6th Petroleum Geology Conference: Geological Society, London, 833–844.

Planke, S., H. Svensen, R. Myklebust, S. Bannister, B. Manton, and L. Lorenz, 2015, Geophysics and Remote Sensing, *in* Advances in Volcanology, Springer, Berlin Heidelberg, 1–16.

Planke, S., P. A. Symonds, E. Alvestad, and J. Skogseid, 2000, Seismic volcanostratigraphy of large-volume basaltic extrusive complexes on rifted margins: Journal of Geophysical Research, **105**, 19333–19351.

Planke S., E. Alvestad, and O. Eldholm, 1999. Seismic characteristics of basaltic extrusive and intrusive rocks: The Leading Edge, 342-348.

Posamentier, H. W., R. J. Davies, J. A. Cartwright, and L. Wood, 2007, Seismic geomorphology-an overview: Geological Society, London, Special Publications, **277**, 1.

Reynolds, P. R., R. J. Brown, T. Thordarson, E. Llewellin, and K. Fielding, 2015, Rootless cone eruption processes informed by dissected tephra deposits and conduits: Bulletin of Volcanology, **77**, 72.

Schiffman, P., R. J. Watters, N. Thompson, and A. W. Walton, 2006, Hyaloclastites and the slope stability of Hawaiian volcanoes: Insights from the Hawaiian Scientific Drilling

This paper presented here as accepted for publication in Interpretation prior to copyediting and composition.
© 2017 Society of Exploration Geophysicists and American Association of Petroleum Geologists.

Project's 3-km drill core: Journal of Volcanology and Geothermal Research, **151**, 217-228.

Schofield, N., and D. W. Jolley, 2013, Development of intra-basaltic lava-field drainage systems within the Faroe–Shetland Basin: Petroleum Geoscience, **19**, 273-288.

Schofield, N., S. Holford, J. M. Millett, D. Brown, D. R. Jolley, S. Passey, D. Muirhead, C. Grove, C. Magee, J. Murray, and M. Hole, 2015, Regional magma plumbing and emplacement mechanisms of the Faroe-Shetland Sill Complex: implications for magma transport and petroleum systems within sedimentary basins: Basin Research, **29**, 41-63. DOI: 10.1111/bre.12164.

Self, S., T. Thordarson, L. Keszthelyi, G. P. L. Walker, K. Hon, M. T. Murphy, P. Long, and S. Finnemore, 1996, A new model for the emplacement of Columbia River basalts as large, inflated pahoehoe lava flow fields: Geophysical Research Letters, **23**, 2689-2692.

Single, R. T., and D. A. Jerram, 2004, The 3D facies architecture of flood basalt provinces and their internal heterogeneity: examples from the Palaeogene Skye Lava Field: Journal of the Geological Society, **161**, 911-926.

Skilling, I.P., 2002, Basaltic pahoehoe-fed lava deltas; large-scale characteristics, clast generation, emplacement processes and environmental discrimination: Geological Society, London, Special Publications, **202**, 91–113.

Smith, J. R., A. Malahoff, and A. N. Shor, 1999, Submarine geology of the Hilina slump and morpho-structural evolution of Kilauea volcano, Hawaii: Journal of Volcanology and Geothermal Research, **94**, 59-88.

This paper presented here as accepted for publication in Interpretation prior to copyediting and composition.
© 2017 Society of Exploration Geophysicists and American Association of Petroleum Geologists.

Stevenson, J. A., N. C. Mitchell, N, Cassidy, and H. Pinkerton, 2011, Widespread inflation and drainage of a pāhoehoe flow field: the Nesjahraun, Þingvellir, Iceland: Bulletin of Volcanology, **74**, 15-31. doi:10.1007/s00445-011-0482-z.

Vail, P. R., and R.M. Mitchum, 1977, Seismic stratigraphy and global changes of sea level, I, Overview: Memoir American Association of Petroleum Geologists, **22**, 51-52.

Watton, T. J., S. Cannon, R. J. Brown, D. A. Jerram, and B. L. Waichel, 2014, Using formation micro-imaging, wireline logs and onshore analogues to distinguish volcanic lithofacies in boreholes: examples from Palaeogene successions in the Faroe–Shetland Basin, NE Atlantic: Geological Society, London, Special Publications, **397**, 173–192.

Watton, T. J., D. A. Jerram, T. Thordarson, and R. J. Davies, 2013, Three-dimensional lithofacies variations in hyaloclastite deposits: Journal of Volcanology and Geothermal Research, **250**, 19-33.

Wright, K. A., R. J. Davies, D. A. Jerram, J. Morris, and R. Fletcher, 2012, Application of seismic and sequence stratigraphic concepts to a lava-fed delta system in the Faroe–Shetland Basin, UK and Faroes: Basin Research, **24**, 91–106.

This paper presented here as accepted for publication in Interpretation prior to copyediting and composition.
© 2017 Society of Exploration Geophysicists and American Association of Petroleum Geologists.

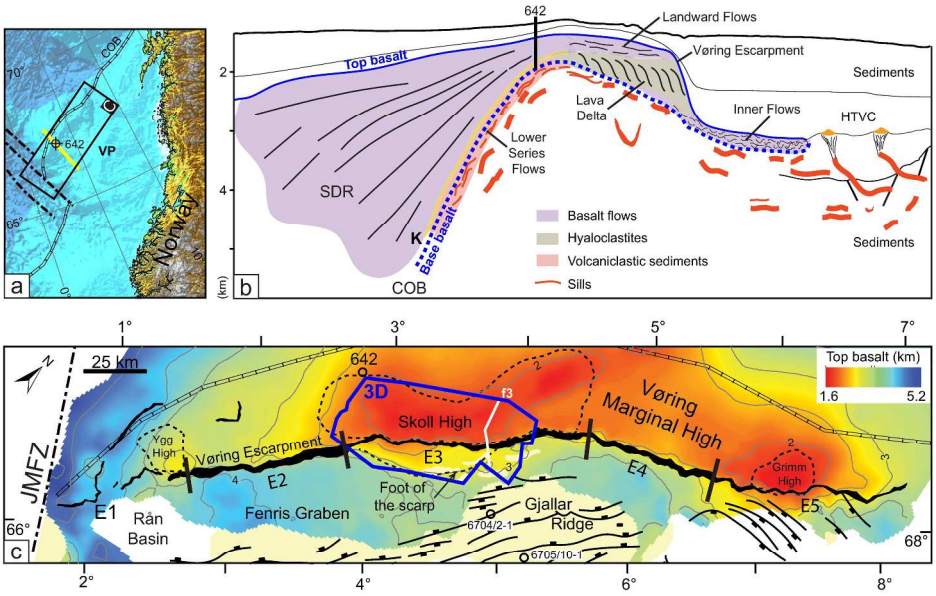

Figure 1

Figure 1. Overview of the volcanic setting of the mid-Norwegian rifted margin and location of the interpreted seismic data. A) Bathymetric map showing the Vøring Plateau (VP), Ocean Drilling Program (ODP) Site 642, and the continent-ocean boundary (COB). B) Schematic cross-section of the Vøring Margin showing characteristic igneous complexes and associated volcanic seismic facies units (Planke et al., 2000). Approximate location shown as yellow line in Figure 1a. C) Regional structural map of the Top basalt horizon on the Vøring Margin slowing the location of the interpreted 3D seismic cube (blue polygon) and P-Cable data (white line, f3). The Vøring Escarpment is divided into five segments, E1 to E5. Structural highs outlined by dashed lines and depth contours in km (gray lines) annotated. Modified from Abdelmalak et al. (2016b). COB: Continent-Ocean Boundary. HTVC: Hydrothermal Vent Complex; K: K-reflection, the base of SDR; SDR: Seaward Dipping Reflectors; VP: Vøring Plateau.

256x330mm (300 x 300 DPI)

This paper presented here as accepted for publication in Interpretation prior to copyediting and composition.
© 2017 Society of Exploration Geophysicists and American Association of Petroleum Geologists.

This paper presented here as accepted for publication in Interpretation prior to copyediting and composition.
© 2017 Society of Exploration Geophysicists and American Association of Petroleum Geologists.

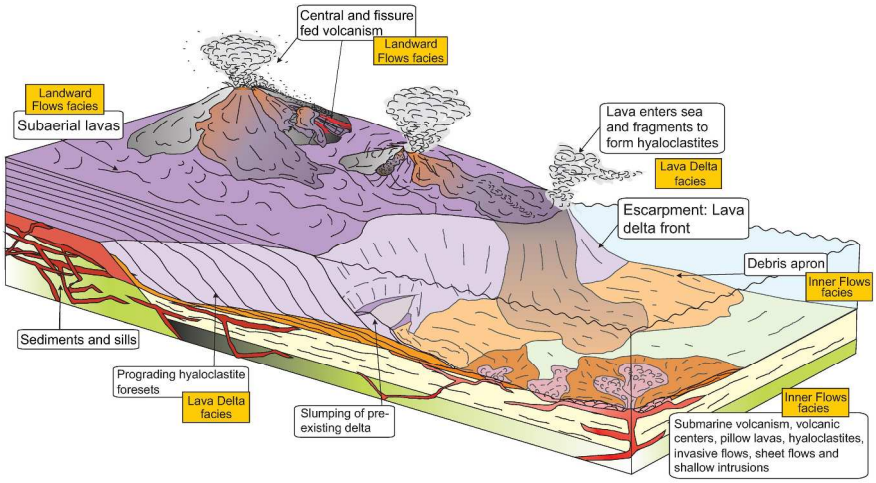

Figure 2

Figure 2. Sketch of volcanic processes and deposits relevant for the Vøring Margin breakup volcanism. Characteristic volcanic seismic facies units (e.g., Inner Flows and Lava Delta) are labeled.

267x368mm (300 x 300 DPI)

This paper presented here as accepted for publication in Interpretation prior to copyediting and composition.
© 2017 Society of Exploration Geophysicists and American Association of Petroleum Geologists.

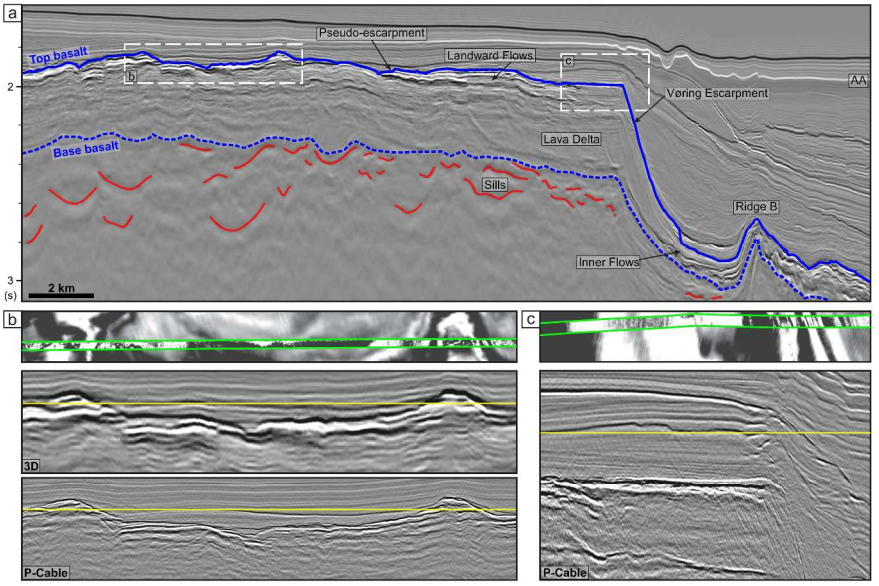

Figure 3

Figure 3. Seismic data examples showing typical data quality. a) Arbitrary seismic profile across the northern part of the 3D survey with interpreted horizons. Line located in Figure 1c. b) Comparison of conventional and high-resolution P-Cable 3D seismic data on the marginal high on time slices (upper panel shows 90 m wide P-Cable swath in green compared with conventional 3D; depth of time slices marked by yellow line below) and seismic sections. c) Vøring Escarpment seismic example, showing comparison of P-Cable and conventional time slices (upper panel; color scheme as in Figure 3b) and P-Cable seismic section (below).

271x375mm (300 x 300 DPI)

This paper presented here as accepted for publication in Interpretation prior to copyediting and composition.
© 2017 Society of Exploration Geophysicists and American Association of Petroleum Geologists.

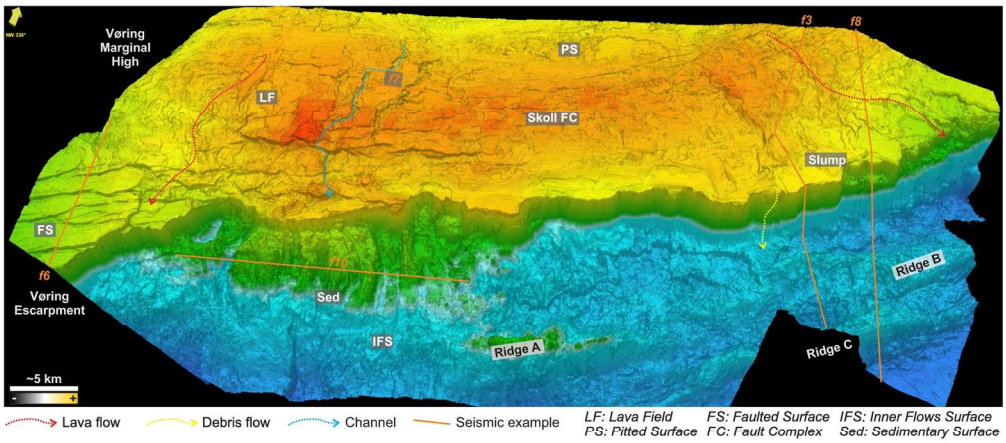

Figure 4a

Figure 4a. Perspective views of the Top basalt horizon. a) Depth and coherency blend. b) Top basalt RMS amplitude and coherency blend (RMS65). Seismic profiles located (f3, f8, f6, f10).

163x104mm (300 x 300 DPI)

This paper presented here as accepted for publication in Interpretation prior to copyediting and composition.
© 2017 Society of Exploration Geophysicists and American Association of Petroleum Geologists.

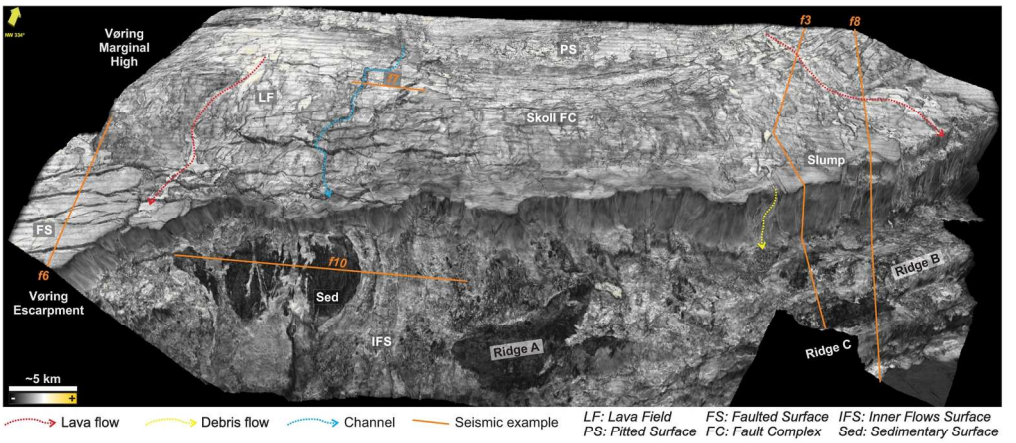

Figure 4b

4b Cont.

163x104mm (300 x 300 DPI)

This paper presented here as accepted for publication in Interpretation prior to copyediting and composition.
© 2017 Society of Exploration Geophysicists and American Association of Petroleum Geologists.

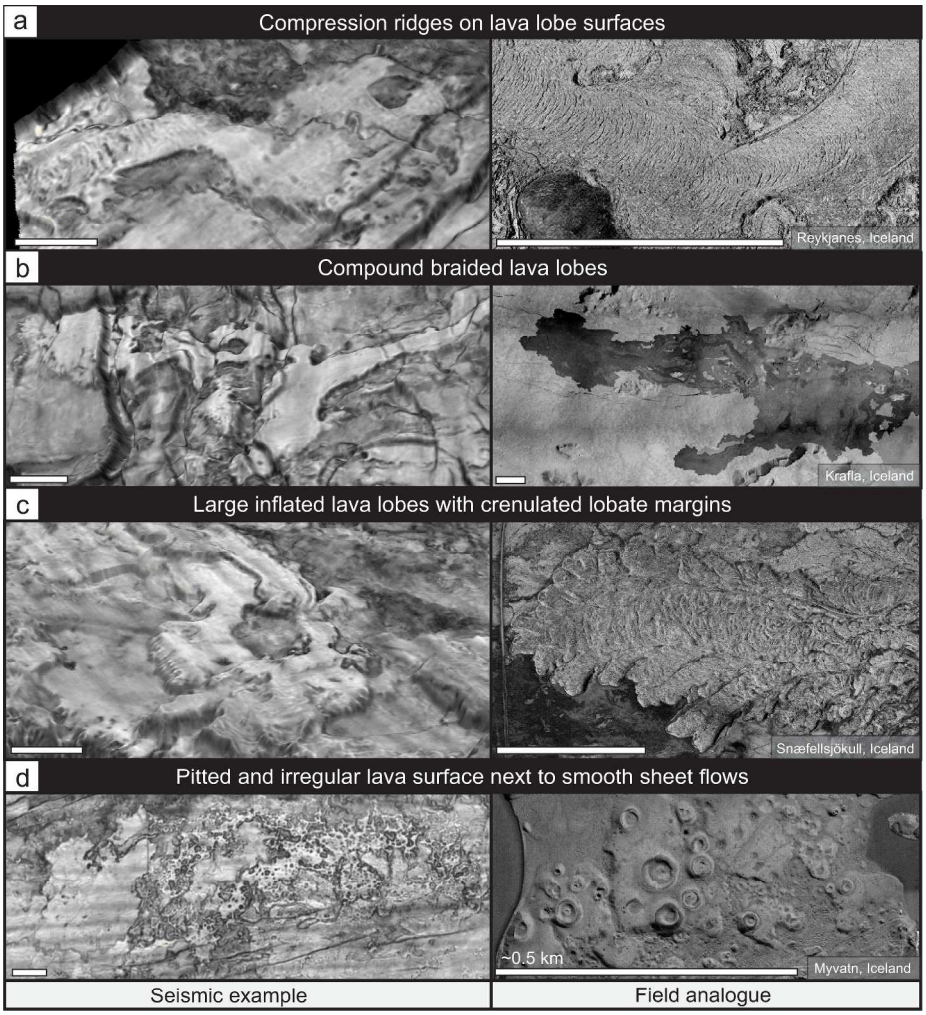

Figure 5

Figure 5. Comparison between seismic lava flow geomorphology of the RMS65 Top basalt horizon with field analogues. a) Compression ridges formed on the surfaces of lava flows indicating flow direction. b) Compound braided lava lobes formed by the eruption of numerous anastomosing flow lobes. c) Large inflated flow lobes with multiple smaller lobes at margins. d) Pitted irregular lava surfaces formed by the formation of rootless cones where lava erupt over a water saturated substrate. All scale bars represent ~1 km unless stated otherwise. Field images from Google Earth.

244x318mm (300 x 300 DPI)

This paper presented here as accepted for publication in Interpretation prior to copyediting and composition.
© 2017 Society of Exploration Geophysicists and American Association of Petroleum Geologists.

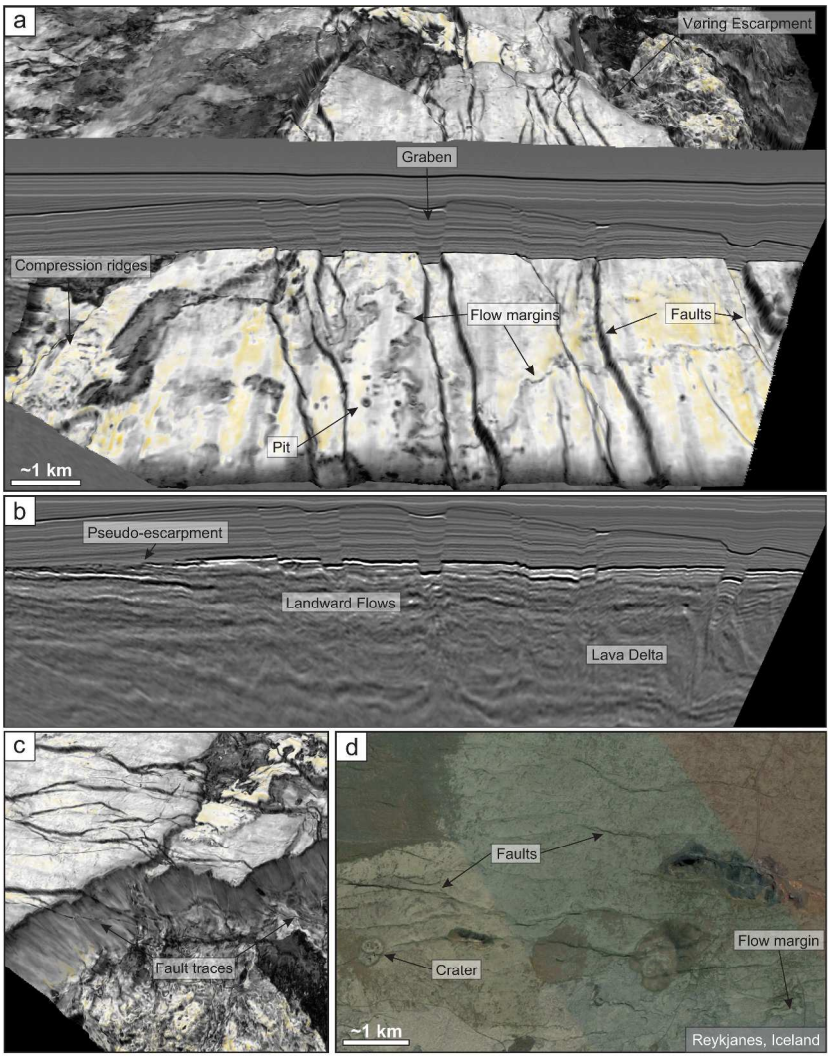

Figure 6

Figure 6. Perspective view of faulted lava fields on the RMS30 Top basalt horizon. a) Grabens dissecting the Skoll High viewed from the south. b) The 2D seismic line in a) showing that the faults cut through the volcanic sequence (Landward Flows and Lava Delta). c) Examples of faults dissecting the Vøring Escarpment and the Inner Flows. View from the north. d) Field analogue of a faulted lava field in a rift zone. Seismic profile located in Figure 4.

280x408mm (300 x 300 DPI)

This paper presented here as accepted for publication in Interpretation prior to copyediting and composition.
© 2017 Society of Exploration Geophysicists and American Association of Petroleum Geologists.

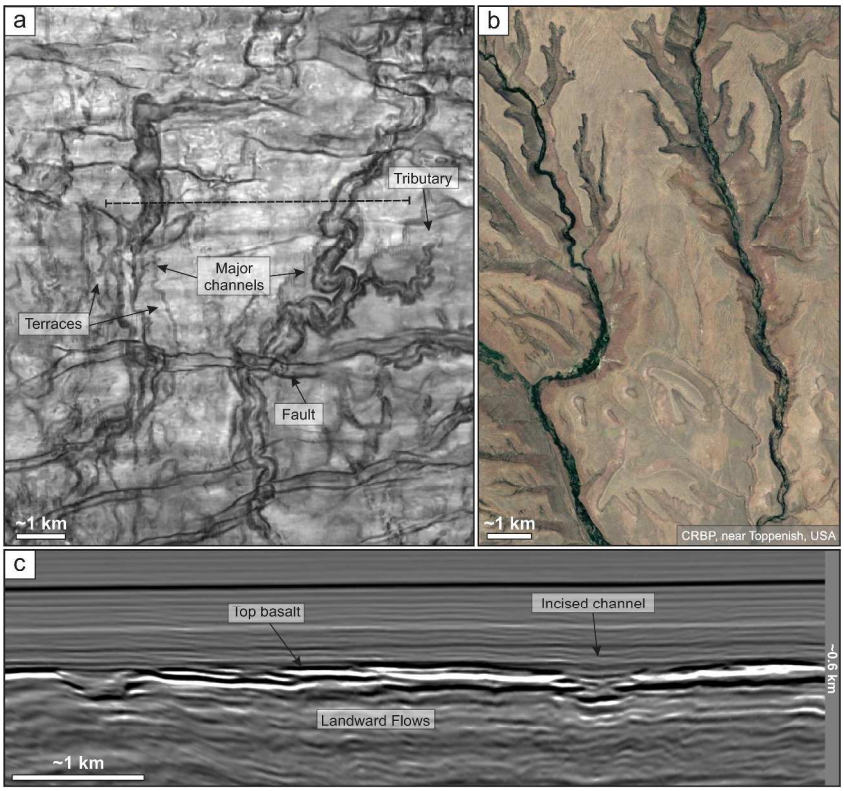

Figure 7

Figure 7. Examples of erosional channels cutting into the top basalt surface. a) Large meandering channels cutting the RMS65 Top basalt horizon. b) Field analogue from the Columbia River Basalt Province (CRBP) where erosional channels incise the lava plateau. c) 2D seismic line showing the discontinuous Top basalt horizon with incised channels. Line located in Figures 4 and 7a.

282x403mm (300 x 300 DPI)

This paper presented here as accepted for publication in Interpretation prior to copyediting and composition.
© 2017 Society of Exploration Geophysicists and American Association of Petroleum Geologists.

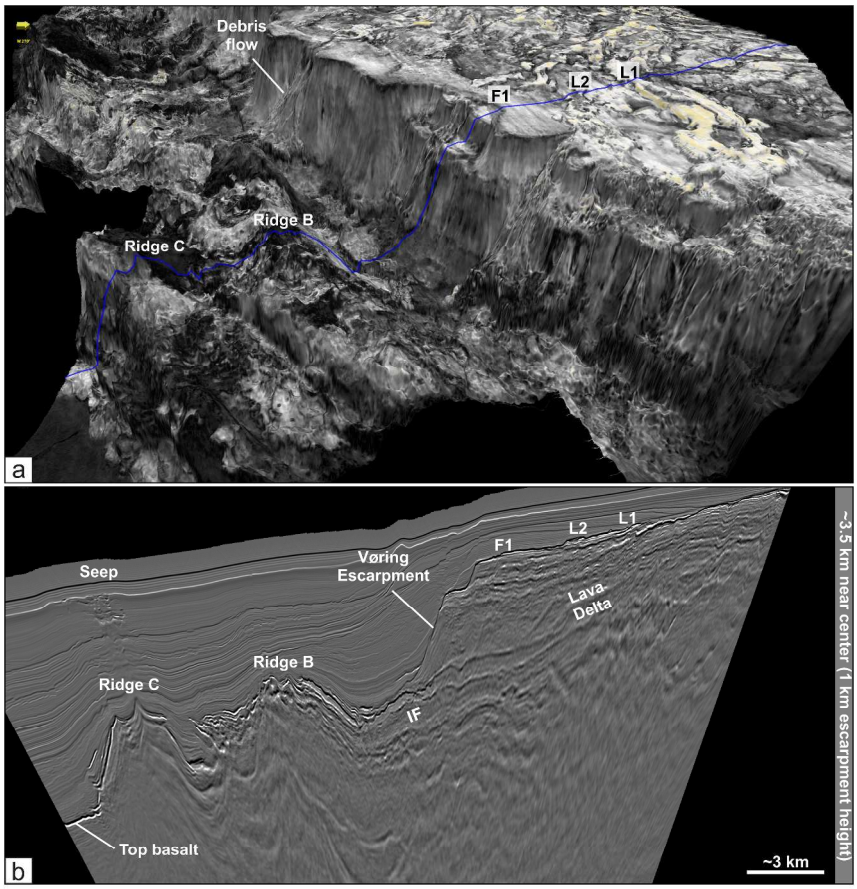

Figure 8

Figure 8. Igneous seismic geomorphology of the Vøring Escarpment. a) Perspective view of the RMS30 Top basalt horizon seen from the north. b) Seismic example along the blue line in a). Location of fault scarp (F1) and lava flows (L1, L2) shown. IF: Inner Flows.

260x367mm (300 x 300 DPI)

This paper presented here as accepted for publication in Interpretation prior to copyediting and composition.
© 2017 Society of Exploration Geophysicists and American Association of Petroleum Geologists.

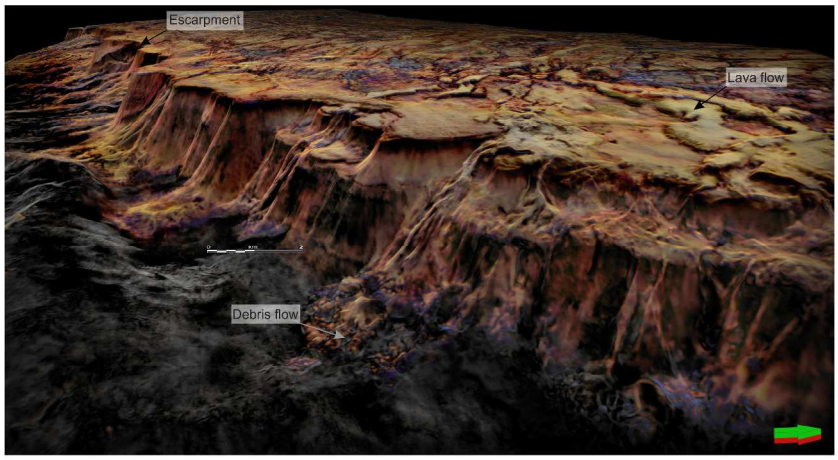

Figure 9

Figure 9. Perspective view of the Vøring Escarpment, looking towards SW. The image displays the interpreted Top basalt horizon blended with coherency data. The image reveals a well-developed subaerial lava field on the Vøring Marginal High and a prominent, about 1 km high, coastal escarpment. Volcanogenic debris flows are identified on the escarpment and spreads out as lobes in the Fenris Graben. Note that the Top basalt horizon is picked at a slightly higher stratigraphic level than in Figure 8 in this part of the cube to better visualize the lower part of the debris flow. Scale bar is approximate for the central part of the figure. The image was generated using the Petrel software.

281x407mm (300 x 300 DPI)

This paper presented here as accepted for publication in Interpretation prior to copyediting and composition.
© 2017 Society of Exploration Geophysicists and American Association of Petroleum Geologists.

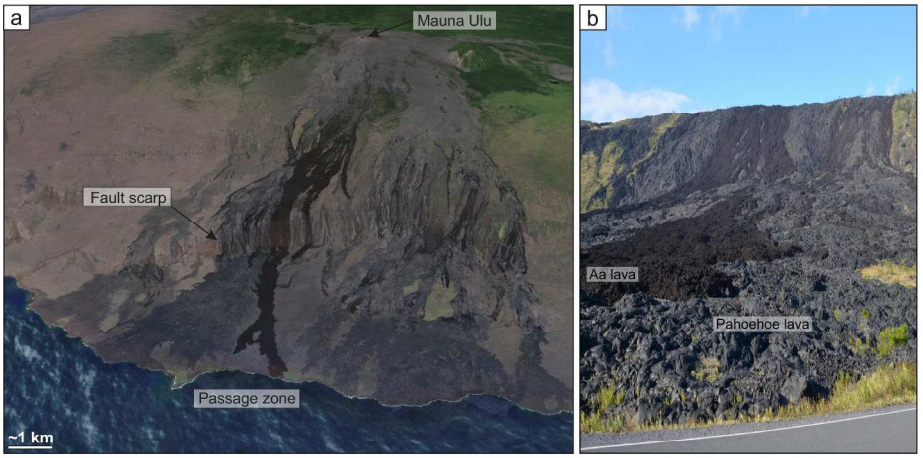

Figure 10

Figure 10. Analogue igneous geomorphology of escarpments in Hawaii. a) Google Earth perspective view of the southern part of Hawaii, showing fault scarps (pali) and recent lava fields. b) Photo of recent lava flows across the fault scarp.

258x339mm (300 x 300 DPI)

This paper presented here as accepted for publication in Interpretation prior to copyediting and composition.
© 2017 Society of Exploration Geophysicists and American Association of Petroleum Geologists.

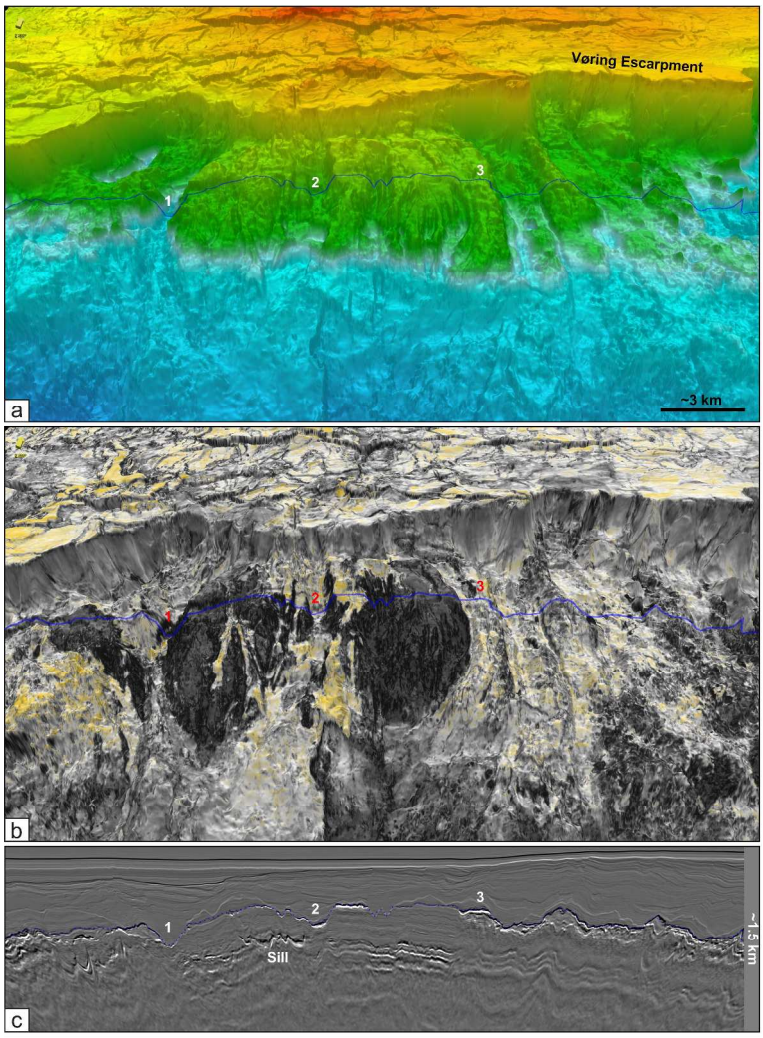

Figure 11

Figure 11. Perspective view of paleo-channels, or valleys, across the Vøring Escarpment. a) Depth horizon of the Top basalt. b) RMS30 Top basalt horizon. c) Seismic strike-line along the central part of the escarpment. Profile located in Figure 4 and as blue line in Figures 10a,b. Numbers 1, 2, and 3 show valleys and ridge. Color scales as in Figure 4.

264x419mm (300 x 300 DPI)

This paper presented here as accepted for publication in Interpretation prior to copyediting and composition.
© 2017 Society of Exploration Geophysicists and American Association of Petroleum Geologists.

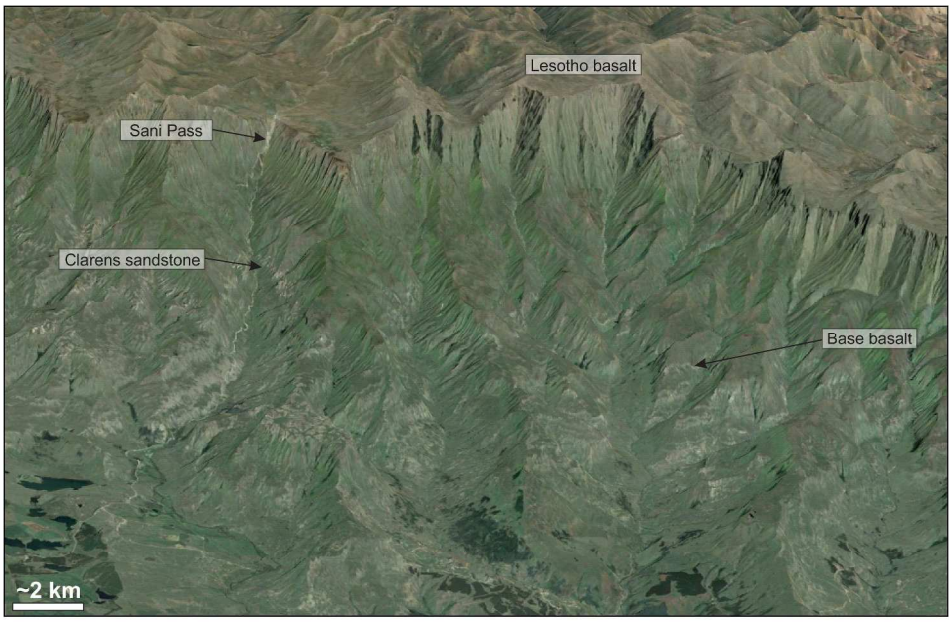

Figure 12

Figure 12. Analogue erosional channels on the southeastern flank of the Lesotho plateau, South Africa. View towards northwest. The elevation of the Sani Pass is from c. 1600-2900 m, with the upper 1000 m comprising lavas overlying the Clarens Sandstone. Image from GoogleEarth.

249x317mm (300 x 300 DPI)

This paper presented here as accepted for publication in Interpretation prior to copyediting and composition.
© 2017 Society of Exploration Geophysicists and American Association of Petroleum Geologists.